ALOS PALSAR verification processor

Pasquali, P ; Monti Guarnieri, A ; D'Aria, D ; Costa, L ; Small, David ; Jehle, Michael ; Rosich, Betlem

Abstract: This paper presents a verification processor, developed under ESA contract, for the generation of polarimetric, interferometric and polarimetric-interferometric geocoded products derived from SAR data obtained from the ALOS PALSAR instrument. The processor, developed with a modular approach, contains the following main elements: - Phase-preserving fine resolution processor; - Phase-preserving ScanSAR processor; - Interference removal tools; - Polarimetric calibration tools; - Polarimetric analysis tools; - Fine resolution interferometric processor; - ScanSAR interferometric processor; - Polarimetric-interferometric processor; - Geocoding; - Atmospheric modelling tools. All of the PALSAR acquisition modes (i.e. stripmap in one, two and full polarisations as well as ScanSAR) are supported both starting from raw and focused data. The processor architecture is presented; highlights are given on modules and algorithms specifically developed for handling the peculiarities of these L-Band SAR data. Examples are shown obtained during the first year of operation of the system, over a number of test sites and of different types of products and acquisition modes.

Originally published at:
Pasquali, P; Monti Guarnieri, A; D'Aria, D; Costa, L; Small, David; Jehle, Michael; Rosich, Betlem (2007). ALOS PALSAR verification processor. In: Envisat Symposium 2007, Montreux (CH), 23 April 2007 - 27 April 2007. European Space Agency * Communication Production Office, online.

ALOS PALSAR VERIFICATION PROCESSOR

P. Pasquali (1), A. Monti Guarnieri (2), D. D'Aria (3), L. Costa (3), D. Small (4), M. Jehle (4) and B. Rosich (5)

(1) sarmap s.a., Cascine di Barico, 6989 Purasca, Switzerland, Email: paolo.pasquali@sarmap.ch
(2) Politecnico di Milano, Piazza Leonardo da Vinci 32, 20133 Milano, Italy, Email: monti@elet.polimi.it
(3) ARESYS s.r.l.,Via Garofalo 39, 20133 Milano, Italy, Email: davide.daria@aresys.it
(4) University of Zürich, Winterthurerstrasse 190 - 8057 Zurich, Switzerland, Email: david.small@geo.unizh.ch
(5) ESA-ESRIN, Via Galileo Galilei - 00044 Frascati, ROMA, Italy, Email: betlem.rosich@esa.int

ABSTRACT

This paper presents a verification processor, developed under ESA contract, for the generation of polarimetric, interferometric and polarimetric-interferometric geocoded products derived from SAR data obtained from the ALOS PALSAR instrument.

The processor, developed with a modular approach, contains the following main elements:

- Phase-preserving fine resolution processor;
- Phase-preserving ScanSAR processor;
- Interference removal tools;
- Polarimetric calibration tools;
- Polarimetric analysis tools;
- Fine resolution interferometric processor;
- ScanSAR interferometric processor;
- Polarimetric-interferometric processor;
- Geocoding;
- Atmospheric modelling tools.

All of the PALSAR acquisition modes (i.e. stripmap in one, two and full polarisations as well as ScanSAR) are supported both starting from raw and focused data.

The processor architecture is presented; highlights are given on modules and algorithms specifically developed for handling the peculiarities of these L-Band SAR data. Examples are shown obtained during the first year of operation of the system, over a number of test sites and of different types of products and acquisition modes.

1 INTRODUCTION

The successful launch of ALOS satellite [1], thanks to the peculiar L-band frequency and full-polarimetric acquisition capabilities of its PALSAR instrument, opens new perspectives in the field of interferometric and polarimetric applications. The PALSAR characteristics and acquisition modes are summarized in Table 1.

A processor has been developed under ESA contract for the verification of the data quality and of potentialities of PALSAR data for different interferometric, polarimetric and polarimetric-interferometric applications.

Table 1. Polarimetric calibration over Corner Reflectors

Mode	Fine Resolution	ScanSAR	Polarimetric (Experimental mode 1)
Center Frequency	1270 MHz		
Bandwidth	28 / 14 MHz		
Polarization	HH or VV / HH+VV or VV+VH	HH or VV	HH+HV+VH+VV
Resolution	10 m (2 look) / 20 m (4 look)	100 m (multi look)	30 m
Swath Width	70 km	250 ~ 350 km	30 km
Incidence Angle	8 ~ 60 degrees	18 ~ 43 degrees	8 ~30 degrees
NE sigma zero	< -23 dB < -25 dB	< -25 dB	< -29 dB
S / A	> 16 dB / > 21 dB	> 21 dB	> 19 dB
Bit length	3 bits / 5 bits	5 bits	3 bits / 5 bits
Antenna Size	Azimuth: 8.9 m, Elevation: 2.9m		

2 SYSTEM OVERVIEW

An overview of the verification processor is shown in 0. A number of modules and packages are available to allow an end-to-end approach, starting from PALSAR raw data up to geocoded products obtained through different techniques.

Phase-preserving fine resolution and ScanSAR processors: an Ω-k approach is used to guarantee the preservation of all phase information, necessary for the sub-sequent processing steps. The ScanSAR phase-preserving processor is particularly innovative, extending all coherent applications to the use of wide-area data [2][3]. As opposed to the products provided by Jaxa, the verification processor delivers Zero-Doppler annotated products.

Interference removal tools are included within the processors due to the high occurrence of interferences in L-Band . A number of approaches are implemented,

Proc. 'Envisat Symposium 2007', Montreux, Switzerland
23–27 April 2007 (ESA SP-636, July 2007)

based on a statistic of the interference types that have been detected in the PALSAR raw data up to now.

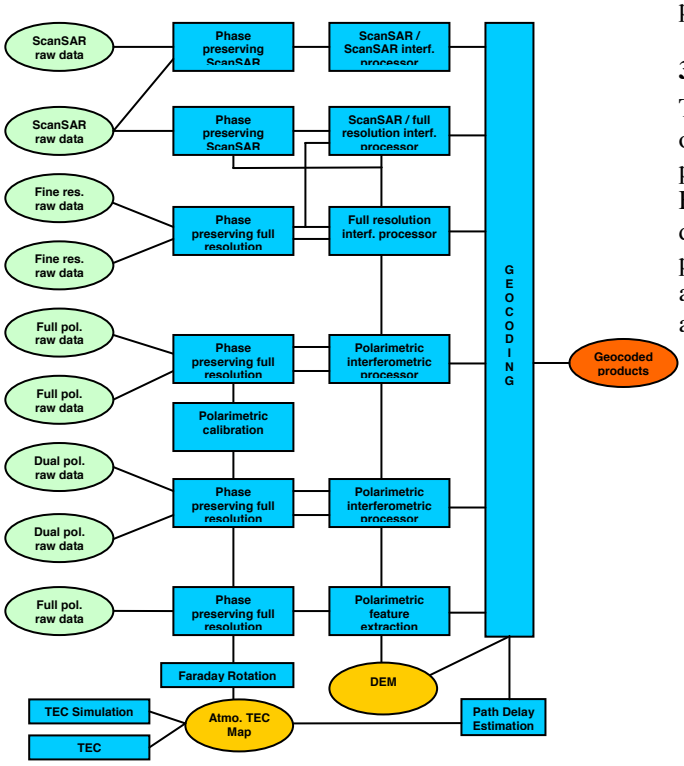

Fig. 1. System overview.

Polarimetric calibration tools allow the correction of system-induced effects and the reconstruction of the real scattering matrix of the imaged areas from the measured one.

Polarimetric analysis tools are provided like polarimetric signature analysis, polarisation synthesis and decomposition, coherence estimation as well as polarimetric classification.

Fine resolution and ScanSAR interferometric processors allow the computation of coherence maps and Digital Elevation models, both from fine resolution or ScanSAR data as well as from combinations of the two types of products.

Polarimetric interferometry modules are provided to perform coherence optimisation based on an adaptive approach as well as perform parameter inversion to obtain information concerning tree heights.

Geocoding; a rigorous approach, based on a DEM and the solution of the Range-Doppler equations of the system is adopted both for the geocoding of the final products and for the generation of the synthetic fringes used during the interferometric processing.

Atmospheric modelling tools: they provide path delay estimates for use in the geocoding step, starting from total electron content (TEC) map estimates describing spatial variations in TEC values across the Earth. These estimates are obtained either from GNSS measurements or from simulations [1].

Estimations of the Faraday Rotation impacting on full-polarimetric data are also obtained from GNSS

3 RESULTS

The following figures present a number of results obtained with the different modules of the verification processor.

Fig. 2 shows the azimuth time – range spectrum distribution of a segment of ALOS raw data. Here it is possible to notice how different types of interferences appear: band & time-limited, single instant tones as well as continuous tones at specific frequencies.

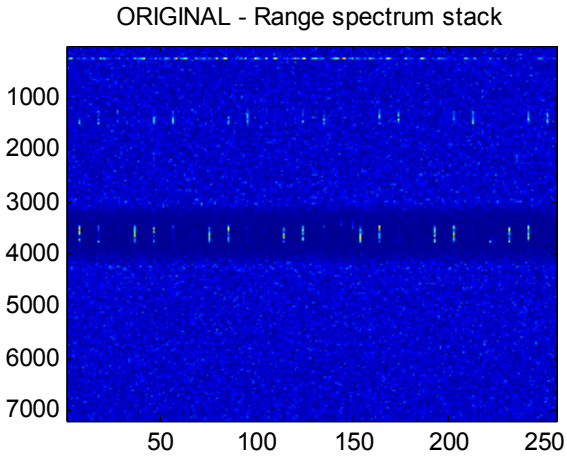

Fig. 2. Azimuth time – range spectrum distribution of a segment of ALOS raw data.

Another type of artefacts detected is shown in Fig. 3. It has been detected that, in some lines after the occurrence of some type of interferences are showing an overall lower value of the spectrum when compared with the expected one as computed from the information on the transmitted chirp power and on the average of the power of the previous lines.

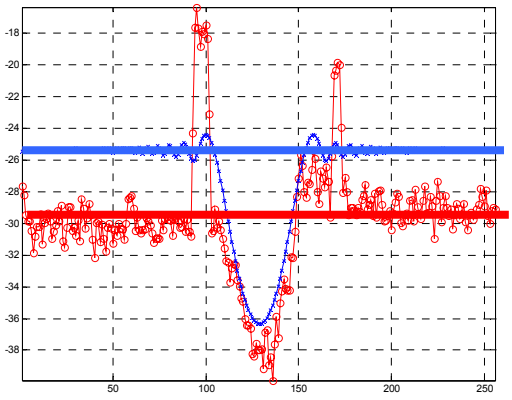

Fig. 3. Power loss effect. Real data range spectrum in red; expected spectrum in blue.

Fig. 4 shows the result of applying some of the implemented approaches to interferences removal, evident when comparing the upper image (not corrected) with the lower one.

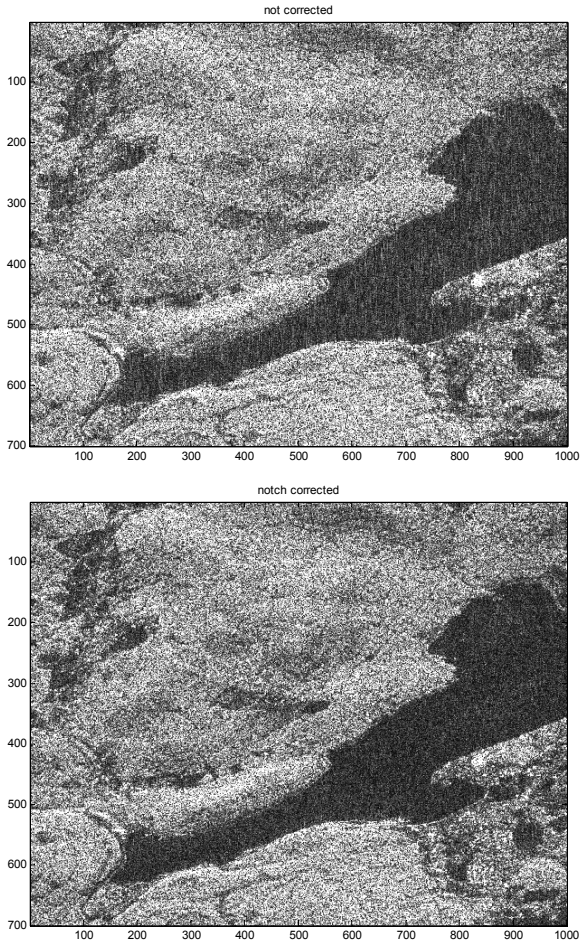

Fig. 4. Interferences removal. Data affected by interferences (above) vs. interference-removed data (below)

Table 2. is showing an evaluation of the polarimetric calibration of full-polarimetric data, as provided by Jaxa and evaluated on the Corner Reflectors installed around the DLR area (Oberpfaffenhofen, Germany).
The results are very promising. The development now concentrates in the integration of the TEC maps obtained from the atmospheric modelling tools into an alternative calibration chain, to help the correction of the Faraday rotation effects, and in a DEM-dependant correction of the Antenna Gain Pattern values to be performed before the polarimetric calibration step.

Table 2. Results of polarimetric calibration over Corner Reflectors.

CR	Shift HH-VV	Power Imbalance HH – VV	Power Imbalance HH – VV (dB)	Phase Imbalance HH – VV (deg)
Etterschlag	DR=0 DA=1/32	0.98	-0.4	0.0007
Gilching	DR=0 DA=-1/32	0.99	-0.1	0.0006
Maising	DR=0 DA=7/32	1.01	0.2	0.006
Tiefenbrunnenn	DR=0 DA=0	0.97	-0.6	0.0003
Unterbrunnenn	DR=1/32 DA=0	0.95	-1.0	-0.0003

The accuracy in the localisation of the PALSAR data that can be obtained based on the provided ancillary information (state vectors) only, without GCPs, has being checked with the support of Corner Reflectors, installed for this project, and other methods.

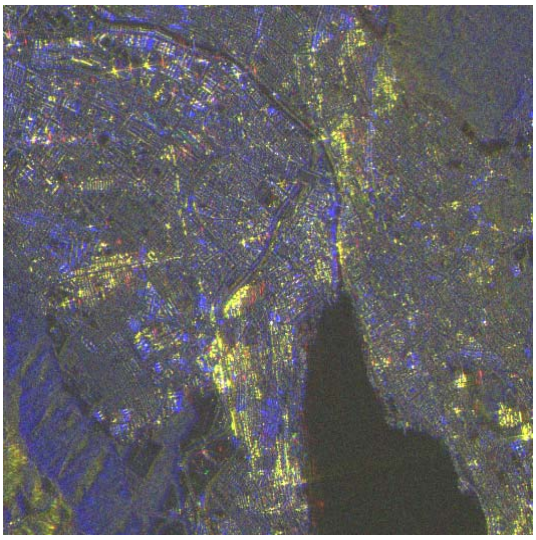

Fig. 5. Multi-temporal overlay in the Zurich region (Switzerland).

Fig. 5 shows an excerpt of a multi-temporal overlay in the Zurich region (CH), obtained by colour-coding one descending and two ascending acquisitions over the same area and geocoded using nominal parameters / ancillary information only. The very good superposition of the different images is clearly visible, even in this case of maximal difference in the acquisition geometry.
Based on the analysis of a number of datasets, an accuracy of around one pixel in the absolute localisation of the Jaxa products can be obtained based on ancillary information only.

After correcting some systematic delays, comparable results are reached with the verification processor.

The accuracy of the orbital information and geometric accuracy of PALSAR data has been checked also against the capability of providing reliable information for the estimation of relative shifts in case of interferometric combination. The results of the shifts as obtained from orbits with the ones obtained by maximising the interferometric coherence are shown in Table 3. It can be seen that the accuracy of the shift parameters obtained from the orbital information, when considering a correct reference height for the area, is in the order of a fraction of a pixel, and particularly good in range direction. These results are of particular interest for the case of ScanSAR interferometry.

Table 2. Comparison between coregistration parameters obtained from the orbital information with those obtained from the SLC data through coherence maximisation.

	Range shift polynomial	Azimuth shift polynomial
Orbital shifts with 600m reference height	364.29 + Rg * 0.0033 – Az * 0.00011	682.94 + Rg * 0.00055 + Az * 0.00356
Coherence maximization	364.26 + Rg * 0.0033 - Az * 0.000097	682.36 + Rg * 0.00054 + Az * 0.00357

One example of a TEC map obtained from GNSS measurements close to the acquisition time of one PALSAR scene is shown in Fig. 6. Depending on the acquisition solar time and solar activity, the availability of such information may allow, in L-Band, to obtain information suitable to correct the absolute location of the products of some tens of metres.

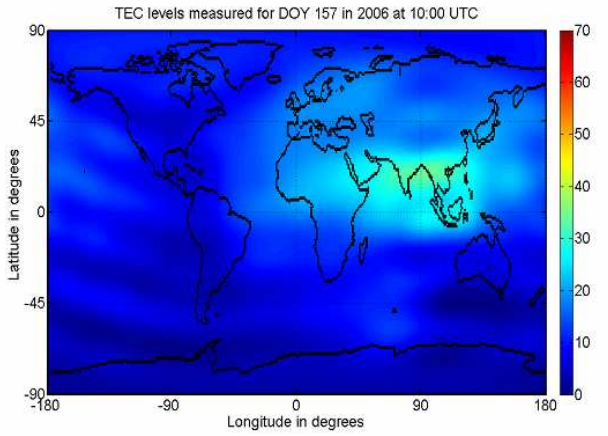

Fig. 6. VTEC map obtained from GNSS measurements close to the acquisition time of one PALSAR scene.

An example of an estimate of the B field at the same time obtained using the IGRF10 model is shown in Fig. 7. A combination of this information allows to obtain an estimate of the impact of the Faraday rotation on a full-polarimetric PALSAR acquisition. Examples of the results obtained over a number of full-polarimetric acquisitions over the Zurich area are shown in Fig. 8 and compared with estimates obtained directly from the SAR data.

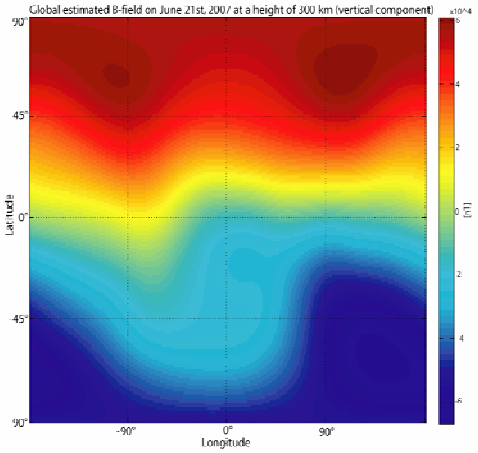

Fig. 7. Vertical component of the B field map obtained from simulations close to the acquisition time of one PALSAR scene.

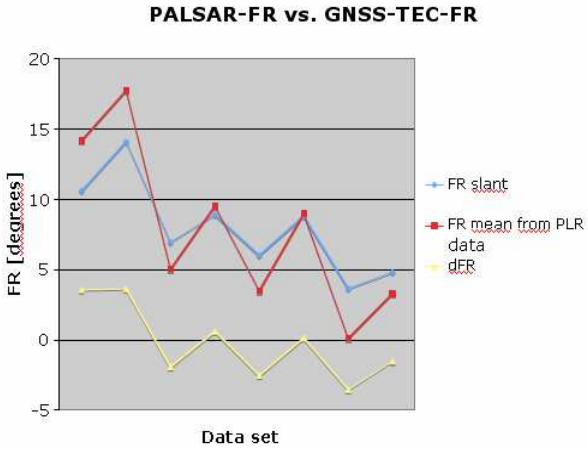

Fig. 8. Faraday rotation estimates as obtained from GNSS and from SAR data.

One example of the results obtained with the Polarimetric Analysis tools on PALSAR data is shown in Fig. 9. The module contains an adaptive implementation of [4].

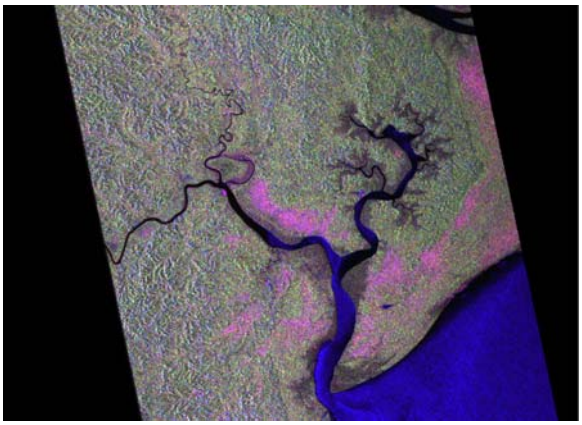

Fig. 9. α-Entropy decomposition of PALSAR data; Irian Jaya (Indonesia).

An example of results obtained with the interferometric processor is shown in Fig. 10 for a test site over Switzerland.

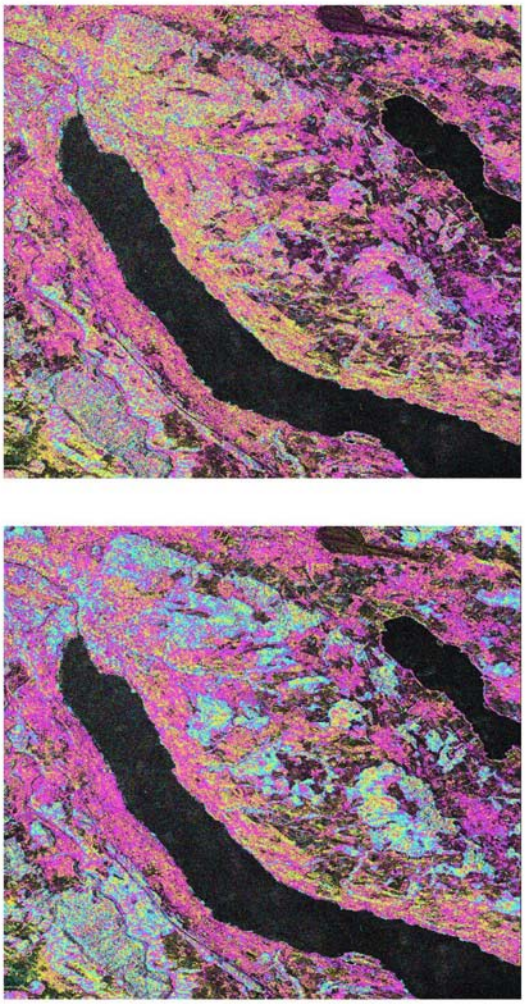

Fig. 10. Comparison between flattening of PALSAR HH interferometric data based on a Digital Terrain Model (above, data copyright of Swisstopo) and on a Digital Surface Model (below, SRTM C-Band data).

Here a comparison between flattening of PALSAR HH interferometric data based on a Digital Terrain Model (above, data copyright of Swisstopo) and on a Digital Surface Model (SRTM C-Band data, below) is shown. A preliminary interpretation of these images is the following:

- HH acquisitions have been processed here, much sensitive to the double-bounce scattering mechanism of the tree trunks.
- This mechanism has a phase centre that corresponds to the centre of the trunk-terrain angle (tree base).
- The contribution of the leaves reflection (maybe already low because of L-band penetration) is quite incoherent with the time, hence filtered away during the interferogram filtering.
- The interferogram then mainly would show the phase of the terrain (close to that obtained from a Digital Terrain Model).
- On the other hand, when subtracting the SRTM phase during the flattening, a almost 0 phase in the non-forest areas (PALSAR ~= SRTM), while a kind of "hole" in the phase is showing up in the forested areas, that corresponds to (the negative of) the tree heights.

A comparison between an extract of the SRTM DEM and of a DEM generated using PALSAR data is shown in Fig. 11. The difference between the spatial resolution is evident here.

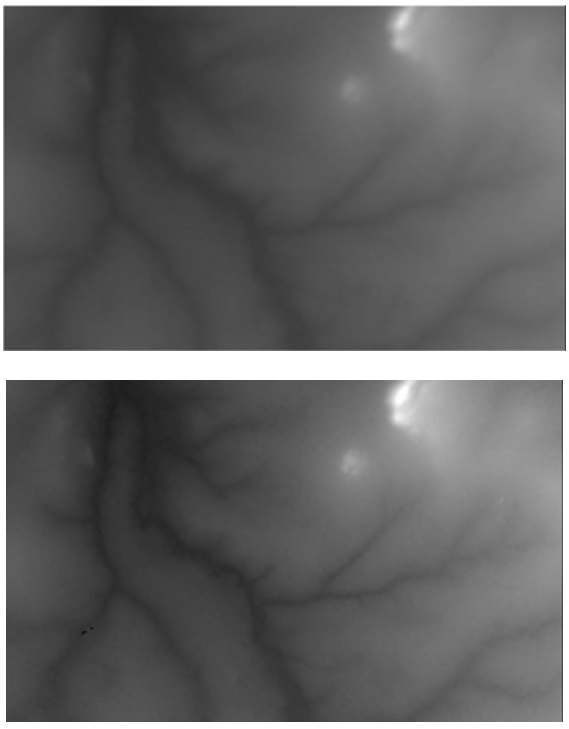

Fig. 11. Comparison between the SRTM (above) and a PALSAR DEM (below); Malawi area.

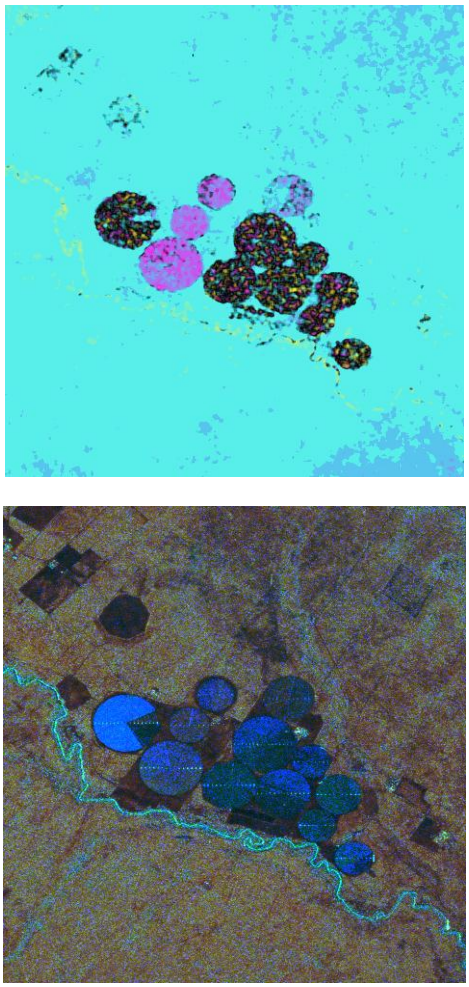

Fig. 12. Interferometric phase (above) and coherence / backscatter / backscatter variation (ILU) false-colour composite (below); Botswana.

An extract of a interferometric phase (above) and coherence / backscatter / backscatter variation (ILU) false-colour composite (below) over Botswana is shown in Fig. 12, showing the different effects of irrigation and agricultural practices on phase, coherence and backscatter.

A multi-temporal colour-composite of three PALSAR acquisitions covering three acquisition cycles is presented in Fig. 13, showing the sensitivity of the data to the growing stage of the agricultural fields.

A number of ScanSAR datasets have been investigated, to identify pairs suitable for interferometric combination. Unfortunately, due to the ALOS on-board mechanism used to select the PRF used during a given acquisition, all the possible pairs showed different PRFs among the same beams, making impossible to obtain burst pattern synchronisation (and hence interferometric capabilities) is not for a very limited number of azimuth lines.

Fig. 13. Multi-temporal colour-composite over Senegal.

4 CONCLUSIONS

The results obtained from ALOS data using the described verification processor are very promising. In particular, they show that very accurate results in terms of processing, interference removal and absolute geolocation of the data may be obtained thanks to the system performances and to a careful processing.

The potentiality of PALSAR data for a number of different land applications seem to be confirmed after the analysis of the data.

5 REFERENCES

1. http://www.eorc.nasda.go.jp/ALOS/
2. A. Monti Guarnieri and C. Prati: "ScanSAR focusing and interferometry", in "*IEEE Transactions on Geoscience and Remote Sensing*", Vol. 34, No. 4, pp. 1029–1038, July 1996.
3. A. Monti Guarnieri and F. Rocca: "Combination of low and high resolution images SAR for differential interferometry", in *"IEEE Transactions on Geoscience and Remote Sensing"*, Vol. 37, No. 3, May 1999.
4. S. Cloude and E. Pottier, "An entropy based classification scheme for land applications of polarimetric SAR," *Geoscience and Remote Sensing, IEEE Transactions on,* Vol. 35, No. 1, Jan. 1997, pp. 68 - 78.
5. M. Jehle, D. Small, E. Meier, D. Nüesch, "Improved Knowledge of SAR Geometry through Atmospheric Modelling", in *"Proceedings of EUSAR 2004"*, Ulm, Germany, May 25-27, 2004, pp. 909-911.